



Matrix optics of artificial intraocular pinhole apertures in astigmatic eyes: modelling depth of field

TANYA EVANS* 

University of Johannesburg, Department of Optometry, Sherwell Street, New Doornfontein, Johannesburg, 2094, South Africa

**tevens@uj.ac.za*

Abstract: This study uses matrix optics to develop a model to predict depth of field in eyes that may have astigmatic elements and apertures that may be elliptical in general. Depth of field is modelled as the visual acuity (VA) as a function of working distance and is illustrated graphically for model eyes that have artificial intraocular pinhole apertures. A small amount of residual myopia is an advantage to increasing the depth of field at near without interfering with distance-vision. A small amount of residual astigmatism is not an advantage to increasing depth of field, without compromising VA at all distances.

© 2023 Optica Publishing Group under the terms of the [Optica Open Access Publishing Agreement](#)

1. Introduction

Over the past two decades, much research and development has gone into finding non-spectacle-based solutions for presbyopia and extended depth-of-focus solutions for cataract patients. Surgically inserted pinhole apertures are one such option. Pinhole optics is based in paraxial optics and a solution that has been used for millennia. AcuFocus (USA) provided two such solutions, the first being the KAMRA corneal inlay [1,2] and the IC-8 IOL the second [3–5]. The Xtrafocus 93 L piggyback phakic intraocular lens (IOL) (Morcher, Germany) was designed for improving the visual acuity (VA) of eyes with optically compromised or irregular corneas but will also give extended depth of field [6,7]. Currently, the possibility of using femto-masking to create an opaque mask with a centered pinhole aperture in any IOL *in-situ* is in the early stages of investigation [8].

The surgically inserted pinhole apertures increase the depth of field, allowing the patient to enjoy distance, intermediate and near vision. Published results for the IC-8 IOL [9], and KAMRA inlay [10] mostly focused on clinical outcomes. The photopic VA results are only presented for three distances; near, intermediate and distance, often as the percentage of participants achieving 6/9.6 (20/32) or better. Depth of field is determined as the dioptric range across which a predetermined acuity is achieved (for example 6/12 across 3.5 D [11]). The refractive status is only available for certain studies [9,10] and is presented as the mean spherical refractive error (MRSE), limiting comparability of the studies. The aim of this paper is to propose a model to illustrate the depth of field in eyes, including eyes with astigmatic elements and apertures or pupils that may be elliptical. The model illustrates graphically the VA, as a smooth continuum, across the entire depth of field, instead of at three predetermined working distances. To create this model, a relationship for VA as a function of working distance is obtained based on blur patch theory [12]. In astigmatic systems, blur patches are elliptical and may be rotated or reflected. An image of an optotype O may be magnified differently along orthogonal meridians, which may be reflected or rotated with respect to the object. This paper extends the prediction of VA, using blur patch theory, to include eyes that are astigmatic. The model includes eyes with pupils that may be elliptical in general or that have a pinhole aperture “surgically inserted”.

2. Methodology: matrix optics

Depth of field is defined as the longitudinal shift in object position without a perceivable loss in visual acuity [12]. The implication of this definition is that the larger the letter size, the greater the depth of field. We, therefore, define depth of field as the range in working distance across which the desired visual acuity is achievable. It is conceivable that different visual acuities are needed for different tasks and at different working distances.

To model depth of field, it is necessary to predict VA. Blur patch theory is one such VA prediction model but is limited to scalar blur ratios. According to blur patch theory, light from a point object entering an ametropic eye will make a blur patch on the retina. In a centered system with rotationally symmetrical refracting elements and circular aperture, the blur patch is circular with diameter P . The size of the blur circle will depend on the amount of defocus and the size of the aperture [12]. Rabbetts [12] defines a blur ratio as

$$BR = \frac{P}{I} \quad (1)$$

where I is the height of the image as determined by tracing the chief rays and ignoring the blur. BR is used to predict the recognition of letters.

The average person can recognise optotypes with a retinal blur ratio of between 0.8 and 1.0 [12]. The closer the blur ratio is to 0, the clearer the image appears. Jacobs *et al.* [13] obtained the ratio of the angular blur disc diameter to minimum angle of resolution, ($ABDD/MAR$) for a range of pinhole apertures and defocus situations. The $ABDD/MAR$ is a ratio based on angles subtended at the nodal point while blur ratio is based on physical dimensions at the retina. The two methods are comparable when one equates the MAR measuring the limb of an optotype [13] to the full length of the line or optotype [12] such that $BR = ABDD/(MAR \times 5)$. For their own experiments, two participants obtained mean equivalent blur ratios of 0.86 and 0.92 [13]. Chan *et al.* [14] applied the calculations from [13] to a dataset and found equivalent blur ratios of between 0.66 and 0.86 with a mean of 0.76. Maximum resolvable blur ratios vary among individuals.

To obtain the depth of field in eyes that may be astigmatic, the blur patch model needs to be generalized so that VA may be predicted in astigmatic eyes.

Geometrical optics is an approximation to wave optics and ignores the wave character of light. This is valid when the various apertures are large compared to the wavelength of light and when one doesn't examine the edges of shadows or foci too closely. Geometrical optics does not account for diffraction, interference and polarization [15]. Linear optics, also known as matrix optics is an approximation to geometrical optics where the approximation of small angles is applied. This approximation was known to Ptolemy. The implication is that all quadratic expressions or higher-order aberrations are ignored [15]. The familiar Gaussian optics is a special case of linear optics where all surfaces are rotationally symmetrical and centred about an optical axis. [15].

A pinhole does not change the reduced vergence of the pencil of light to create a focus on the retina of an ametropic eye. Instead, it reduces the size of the blur patch, making the image appear clearer [16]. A pinhole aperture restricts a pencil of light to only the paraxial rays, making paraxial or first-order optics ideal for the study of pinholes. The study is extended to include eyes that have astigmatic surfaces and apertures that may be elliptical in general and therefore matrix or linear optics is well suited to this study. In order to concentrate on the role of astigmatism, the matrix method is applied. This implies that all the limitations of first-order optics apply to the model and, therefore, higher-order aberrations and diffraction are ignored. The model does not account for the reduction in retinal irradiance caused by the pinhole aperture, especially in low lighting conditions which may affect clinical results and patient satisfaction.

2.1. Generalizing the retinal blur ratio

The retinal blur ratio [Eq. (1)] needs to be generalized for astigmatic systems. The retinal blur patch is the aperture referred to the retina [17]. In an astigmatic system the retinal blur patch (subscript R, superscript P) is elliptical in general and is represented by the generalized radius \mathbf{R}_R^P instead of diameter P [18]. \mathbf{R}_R^P is the 2×2 matrix whose eigenvalues represent the major and minor semi-lengths of an ellipse and fulfils the definition of a vector space. Similarly, instead of merely considering the height of the object and image, the object is defined as an elliptical optotype, such as the letter O. The chief rays define the position of the image and therefore the geometry of the aperture does not influence the image. The retinal image (superscript I) is represented by generalized radius \mathbf{R}_R^I and is the object \mathbf{R}_{O+} , a generalized radius, referred to the retina.

Division is not defined in linear algebra. To generalize the retinal blur ratio for astigmatic systems, Eq. (1) is rewritten as $BR(I) = P$, which represents the blur ratio BR as an operator, and generalizes to $\mathbf{M}_{BR}\mathbf{R}_R^I = \mathbf{R}_R^P$. The 2×2 generalized retinal blur ratio is, therefore,

$$\mathbf{M}_{BR} = \mathbf{R}_R^P(\mathbf{R}_R^I)^{-1} \quad (2)$$

Linear or matrix optics is used to first obtain relationships for \mathbf{R}_R^P and \mathbf{R}_R^I before returning to interpret generalized radii, referred apertures and objects, the retinal blur ratio and obtain a relationship for VA.

An aperture restricts the pencil of rays coming from an object so that only the rays that pass through the aperture reach the retina. The aperture is therefore referred to the retina and depends on the longitudinal position and geometry of the aperture, along with the optics of the system. An aperture has the effect of splitting a system into two parts, an anterior part upstream of the aperture plane and a posterior part downstream of the aperture plane.

In Fig. 1 the system S_{OE} is defined as from T_O , the plane immediately downstream of the object, to the transverse plane T_R , immediately upstream of the retina. The aperture plane T_P divides S_{OE} into an anterior subsystem S_{OA} and posterior subsystem S_B . Entrance plane T_O is a distance z_O in front of T_K , the transverse plane immediately upstream of the cornea. Informally, T_K and T_R may be referred to as the corneal and retinal planes, respectively. From an object point on T_O with transverse position \mathbf{y}_O , a ray is traced through the pupil or aperture to the retina. Its transverse positions (or simply positions) in the pupil and at the retina are \mathbf{y}_P and \mathbf{y}_R , respectively. A pencil of rays from an object point is restricted by the aperture with geometry \mathbf{R}_{P+} and forms a blur patch on the retina with geometry \mathbf{R}_R^P [19].

A centred optical system may have elements that are astigmatic and are represented by a 4×4 transference [20]

$$\mathbf{S} = \begin{pmatrix} \mathbf{A} & \mathbf{B} \\ \mathbf{C} & \mathbf{D} \end{pmatrix} \quad (3)$$

where \mathbf{A} the *dilation*, \mathbf{B} the *disjugacy*, \mathbf{C} the *divergence* and \mathbf{D} the *divarication* are the fundamental first-order optical properties of the system [21,22]. Each of \mathbf{A} , \mathbf{B} , \mathbf{C} and \mathbf{D} is a 2×2 submatrix. \mathbf{B} has units of length, \mathbf{C} has units of inverse length such as dioptres and \mathbf{A} and \mathbf{D} are unitless. The power of the optical system is obtained from the transference as $\mathbf{F} = -\mathbf{C}$. The transference is also known as the *system matrix* [21–24], *ray transfer matrix* [21,25] or *ABCD matrix* [21,26].

An optical system such as the eye comprises of a number of elementary systems. The transference of a centered astigmatic refracting surface is $\mathbf{S} = \begin{pmatrix} \mathbf{I} & \mathbf{O} \\ -\mathbf{F} & \mathbf{I} \end{pmatrix}$, where \mathbf{I} is the 2×2 identity matrix and \mathbf{O} is the 2×2 null matrix. \mathbf{F} is a symmetric 2×2 dioptric power matrix and

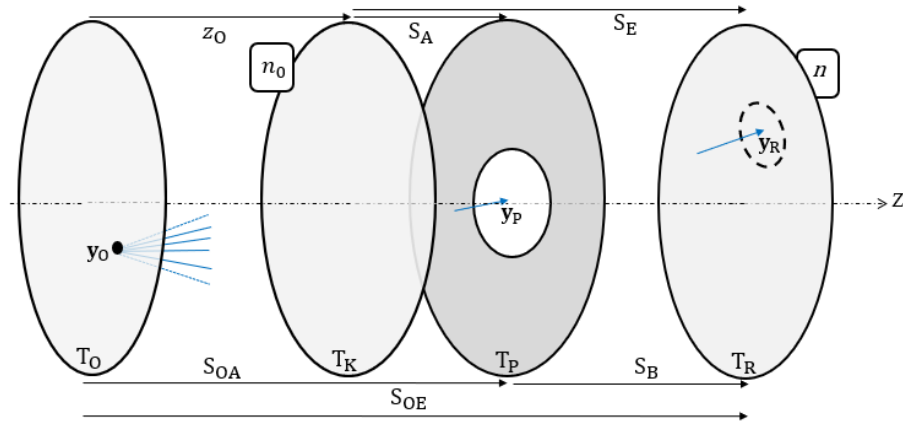


Fig. 1. The super-system S_{OE} of the working distance gap z_O and eye S_E from an object immediately downstream of transverse plane T_O to immediately before the retina at T_R . The anterior super-system S_{OA} includes $z_O > 0$ and anterior eye S_A , up to the aperture plane T_P . The posterior subsystem S_B is shown as from T_P to T_R . A single ray is traced through the eye from the object at T_O with position y_O , reaching the cornea with inclination α_K (not shown), through the aperture with position y_P and reaching the retina with position y_R . The aperture is referred downstream to the retina with blur patch shown by dashed ellipse. Refractive index n_0 is upstream of the eye and n is downstream of T_R .

is described in more detail below. The transference of a homogenous gap is $\mathbf{S} = \begin{pmatrix} \mathbf{I} & \zeta \mathbf{I} \\ \mathbf{O} & \mathbf{I} \end{pmatrix}$

where $\zeta = z/n$, the reduced distance and $\zeta \mathbf{I}$ is a scalar matrix. Let system S_1 have transference \mathbf{S}_1 and similarly for S_2, S_3 , etc. The transference of a compound system made up of a series of m juxtaposed systems $S_1 S_2 S_3 \cdots S_m$ is $\mathbf{S} = \mathbf{S}_m \cdots \mathbf{S}_3 \mathbf{S}_2 \mathbf{S}_1$ [21,27,28], Multiplication is in reverse.

To obtain the transference of the super-system S_{OE} we multiply in reverse [21,27,28] to obtain

$$\mathbf{S}_{OE} = \mathbf{S}_E \mathbf{S}_O = \begin{pmatrix} \mathbf{A}_E & \mathbf{B}_E \\ \mathbf{C}_E & \mathbf{D}_E \end{pmatrix} \begin{pmatrix} \mathbf{I} & \zeta_O \mathbf{I} \\ \mathbf{I} & \mathbf{O} \end{pmatrix} = \begin{pmatrix} \mathbf{A}_E & \zeta_O \mathbf{A}_E + \mathbf{B}_E \\ \mathbf{C}_E & \zeta_O \mathbf{C}_E + \mathbf{D}_E \end{pmatrix} \quad (4)$$

where \mathbf{S}_E is the transference of the eye and \mathbf{S}_O is the transference of the elementary system of the working distance gap z_O . $\zeta_O = z_O/n_0$ is the reduced distance. The transverse plane T_P of the iris and pupil or pinhole aperture divides the system into an anterior subsystem S_{OA} and posterior subsystem S_B (Fig. 1). The anterior subsystem S_{OA} , where \mathbf{S}_A is the transference of the subsystem of the anterior eye, is given by Eq. (3) with subscript E substituted by subscript A throughout [19]. When an aperture such as the KAMRA, IC-8 or Xtrafocus is inserted into the eye, the aperture-plane is no longer coincidental with the iridial-plane and the subsystems S_{OA} and S_B will adjust accordingly.

At transverse planes T_O , T_P and T_R a ray traced through the system has ray states \mathbf{p}_O , \mathbf{p}_P and \mathbf{p}_R , respectively. The ray state at a transverse plane T relative to longitudinal axis Z is a 4×1 matrix given as $\mathbf{p} = \begin{pmatrix} \mathbf{y}^T & \boldsymbol{\alpha}^T \end{pmatrix}^T$ where \mathbf{y} is a position vector with horizontal and vertical Cartesian coordinates $\mathbf{y} = \begin{pmatrix} y_1 & y_2 \end{pmatrix}^T$ and similarly $\boldsymbol{\alpha} = n\mathbf{a}$ is the reduced inclination vector [21]. Superscript T represents the matrix transpose.

To study the geometry of the referred aperture and object, relationships for the position of the ray at each of the three transverse planes are needed, that is, the object plane T_O , aperture

plane T_P and image plane, usually the retina T_R . The basic equation of matrix optics [23,29], is applied across S_{OA} , that is $S_{OA}\rho_O = \rho_P$, and multiplied out to obtain the two matrix equations

$$A_{OA}y_O + B_{OA}\alpha_O = y_P, \quad (5)$$

and

$$C_{OA}y_O + D_{OA}\alpha_O = \alpha_P. \quad (6)$$

Similarly, the ray state across S_B is traced from T_P to T_R such that $S_B\rho_P = \rho_R$, to obtain

$$A_By_P + B_B\alpha_P = y_R. \quad (7)$$

Equation (5) is solved for α_O , substituted into Eq. (6) and simplified using the third Schur complement (a result of symplecticity, see [30]) and then substituted into Eq. (7) to obtain

$$(A_BB_{OA} + B_BD_{OA})B_{OA}^{-1}y_P - B_BB_{OA}^{-T}y_O = y_R. \quad (8)$$

The transference for S_{OE} is

$$S_{OE} = S_BS_{OA} = \begin{pmatrix} A_B & B_B \\ C_B & D_B \end{pmatrix} \begin{pmatrix} A_{OA} & B_{OA} \\ C_{OA} & D_{OA} \end{pmatrix} = \begin{pmatrix} \bullet & A_BB_{OA} + B_BD_{OA} \\ \bullet & \bullet \end{pmatrix}. \quad (9)$$

Entries that are not needed are indicated with \bullet . B_{OE} (the disjugacy B for the system of object and eye, subscript OE) is substituted from Eq. (9) into Eq. (8) to obtain

$$B_{OE}B_{OA}^{-1}y_P - B_BB_{OA}^{-T}y_O = y_R \quad (10)$$

which is rewritten as

$$W_{OE}y_P + X_{OE}y_O = y_R \quad (11)$$

where

$$W_{OE} = B_{OE}B_{OA}^{-1} \quad (12)$$

is the image blur coefficient and

$$X_{OE} = -B_BB_{OA}^{-T} \quad (13)$$

is the image size coefficient for an object at a finite position [31]. Equation (11) traces a ray from a finite object with transverse position y_O , at longitudinal distance z_O from T_O to T_K , through the pupil or aperture with specified transverse position y_P to reach the retina with transverse position y_R . The aperture plane T_P divides the supersystem into two parts (Fig. 1). Any change in the longitudinal position of the aperture, such as the implantation of a pinhole aperture, will have the effect of redefining the anterior and posterior subsystems, and hence, change the values of B_{OA} and B_B . Any change to z_O will change the values of B_{OE} and B_{OA} .

W_{OE} (Equation (12)) and X_{OE} (Eq. (13)) are ratios that are unitless and are made up of the disjugacies of the system S_{OE} and the two subsystems S_{OA} and S_B . A disjugate system is one that is not conjugate, that is, the object is not conjugate with an image on the retina. Where there is a point image on the retina, then $B_{OE} = O$.

From Fig. 1, the working distance z_O is included in each of B_{OE} and B_{OA} . Consider an axial object point such that $y_O = o$ (the null vector) and a pupil with vectorial diameter $\Delta y_P = y_{P2} - y_{P1}$ where y_{P1} and y_{P2} are diametrically opposite each other. The vectorial diameter of the blur patch on the retina will be $W_{OE}\Delta y_P = \Delta y_R$. W_{OE} operates on Δy_P such that Δy_R is magnified and rotated with respect to Δy_P . The diameter of the pupil Δy_P along a chosen meridian is magnified by W_{OE} to create a blur patch on the retina with diameter Δy_R . Δy_R may have been rotated or reflected with respect to Δy_P .

In the same way, a chief ray ($\mathbf{y}_P = \mathbf{o}$ for a centred system) is traced from two object points a transverse vectorial separation $\Delta\mathbf{y}_O$ apart to create an image of size $\mathbf{X}_{OE}\Delta\mathbf{y}_O = \Delta\mathbf{y}_R$ on the retina. \mathbf{X}_{OE} operates on $\Delta\mathbf{y}_O$ to obtain corresponding image vector $\Delta\mathbf{y}_R$ on the retina. $\Delta\mathbf{y}_R$ may be magnified and rotated or reflected with respect to the object $\Delta\mathbf{y}_O$. While this interpretation gives insight into Eq. (11), it is, however, limited.

2.2. Generalized radius of an aperture

The pupil and indeed most apertures may be treated as elliptical. The equation for an ellipse is $x^2/a^2 + y^2/b^2 = 1$ or $\mathbf{r}^T \mathbf{A} \mathbf{r} = 1$ where $\mathbf{r} = \begin{pmatrix} x & y \end{pmatrix}^T$ is a radial vector of the ellipse. The positive eigenvalues of \mathbf{A} are $1/a^2$ and $1/b^2$. \mathbf{A} represents the geometry of the ellipse, that is, the size, shape and orientation of the ellipse. \mathbf{A} is positive definite, that is, both eigenvalues are positive and is undefined if a and/or b are zero. \mathbf{A} , therefore, does not represent a vector space [18].

The generalized radius \mathbf{R} is related through $\mathbf{R} = \mathbf{A}^{-1/2}$. \mathbf{R} is a 2×2 matrix that may have two real distinct eigenvalues, a and b , when the discriminant of \mathbf{R} is positive ($\text{disc}\mathbf{R} > 0$), a unique, real eigenvalue when $\text{disc}\mathbf{R} = 0$ and distinct, complex eigenvalues when $\text{disc}\mathbf{R} < 0$. When \mathbf{R} has rank 2, it may be positive definite where $a, b > 0$, negative definite where $a, b < 0$ and indefinite where $a < 0, b > 0$ or $a > 0, b < 0$. When \mathbf{R} has rank 1 it may have $a = 0$ or $a = b = 0$ which allows for singularities and when \mathbf{R} has rank 0, it has $b = 0$ or $\mathbf{R} = \mathbf{O}$ (the null matrix) [18].

When \mathbf{R} represents a blur patch, rank 2 implies patches that are rotated or reflected, rank 1 implies line foci and rank 0 implies a point focus. A circle is a special case of an ellipse where $|a| = |b|$ and $\text{disc}\mathbf{R} = 0$. \mathbf{A} is undefined at a point or line focus. As a convention the generalized radius of an elliptical aperture \mathbf{R}_{P+} is taken as positive definite (subscript +) and all referred apertures, such as a blur patch, are interpreted with respect to the aperture. In addition, a cross-section of rays that is diverging will have a positive angular radius, while converging rays will have a negative angular radius. The indefinite form of \mathbf{R} is found in the interval of Sturm, between the two line foci [18].

2.3. Obtaining the generalized radii for the image and blur patch

The generalized radius of the blur patch is the aperture referred to the retina and is given as

$$\mathbf{R}_R^P = \mathbf{W}_{OE} \mathbf{R}_{P+} . \quad (14)$$

\mathbf{R}_R^P is a referred aperture and is the cross-section of the restricted pencil at the retinal plane. $\mathbf{W}_{OE} \mathbf{R}_{P+}$ is a fixed contribution by the eye and depends on the refracting elements, separations, longitudinal position and geometry of the pupil or aperture and the longitudinal position of the object. \mathbf{R}_R^P is described by a 2×2 generalized radius and may be asymmetric, positive semi-definite ($a, b \geq 0$), negative semi-definite ($a, b \leq 0$), indefinite, singular or null. \mathbf{R}_R^P may have rank 2, 1 or 0. A conjugate system fulfils the condition $\mathbf{B} = \mathbf{O}$ [21,23]. From Eq. (12), it is possible that the object will form a point focus on the retina such that $\mathbf{B}_{OE} = \mathbf{O}$ and hence $\mathbf{R}_R^P = \mathbf{O}$ (rank 0), implying no blur. When a line focus is positioned on the retina, \mathbf{B}_{OE} will be singular with rank 1. If \mathbf{R}_R^P is symmetric, the semi-lengths and orientations of the orthogonal principal meridians (a and b) are described by its eigenstructure. If \mathbf{R}_R^P is asymmetric, then it is described by a positive definite, symmetric 2×2 matrix followed by a rotation or reflection [18].

Similarly, if an optotype \mathbf{O} (the object) is taken and defined as an ellipse (or circle) with positive definite generalized radius \mathbf{R}_{O+} , then the generalized radius of the image at the retina is

$$\mathbf{R}_R^I = \mathbf{X}_{OE} \mathbf{R}_{O+} . \quad (15)$$

Within the limits of visual resolution, \mathbf{R}_{O+} is always chosen to be positive definite (hence, non-singular). From Eq. (13) it is unlikely that \mathbf{X}_{OE} will be singular for the system of an eye and

a near object. (For singularity one would need a focus (either a point or line focus) in the plane of the aperture to create conjugacy with the object for S_{OA} or conjugacy between the aperture and the retina for S_B which are highly unlikely [22].) Indeed, \mathbf{X}_{OE} is usually negative definite (that is $\det \mathbf{X}_{OE} < 0$). \mathbf{R}_R^I is not necessarily symmetric [Eq. (15)], however, it is negative definite and non-singular (because $\det(\mathbf{AB}) = \det \mathbf{A} \det \mathbf{B}$ [32]). The geometry of the image depends on the object size and position, the eye and longitudinal position of the pupil or aperture. The image, therefore, may undergo magnification of differing amounts along the principal meridians and may undergo reflection. Whilst reflection is expected because the image on the retina is inverted, the reflection is not necessarily exactly about 180° . The elliptical image may appear to be rotated slightly with respect to the object.

2.4. Magnification

Where scalar magnification (m) magnifies an image equally in all directions, a 2×2 matrix magnification \mathbf{M} may magnify differently along the two eigenmeridians of \mathbf{M} . It is possible to have a combination of magnification and minification, upright and inverted and possibly null magnification along one or both of the two eigenmeridians of the generalized magnification matrix \mathbf{M} . This implies that the matrix being magnified may undergo rotation or reflection in addition to magnification and/or minification. In addition, \mathbf{M} may be asymmetric which is interpreted using polar decomposition, that is, to use two successive magnifications; first a positive definite matrix using symmetrisation followed by a rotation or reflection [19,33].

2.5. Generalized retinal blur ratio

The generalized blur ratio for eyes with astigmatic elements [Eq. (2)], $\mathbf{M}_{BR} = \mathbf{R}_R^P \mathbf{R}_R^{I-1}$ is a ratio of the generalized radii of two ellipses. \mathbf{M}_{BR} is interpreted as a positive definite matrix $\mathbf{M}_{BR} +$ followed by a rotation \mathbf{R}_θ or reflection $\bar{\mathbf{R}}_\theta$ matrix, similar to the interpretation of generalized magnification [19,33]. The generalized blur ratio only considers the geometry of the image \mathbf{R}_R^I [Eq. (15)] and blur patch \mathbf{R}_R^P [Eq. (14)] and not their position and for this reason centred systems have been used [21].

Visual acuity in astigmatic eyes is well documented [34–36]. The generalized blur ratio [Eq. (2)] quantifies how blurred a letter appears to the eye. The blur component $\mathbf{W}_{OE} \mathbf{R}_{P+}$ is a fixed contribution by the eye and depends on refracting elements, separations, position and geometry of the pupil or other aperture and the longitudinal position of the target. The image geometry $\mathbf{X}_{OE} \mathbf{R}_{O+}$ depends on the object size and longitudinal positions of the object and aperture and the eye. The blur ratio has three variables, object geometry \mathbf{R}_{O+} , aperture geometry \mathbf{R}_{P+} and working distance z_O . The contribution of an eye remains fixed for a particular aperture plane, assuming no accommodation. The working distance z_O is incorporated in \mathbf{W}_{OE} and \mathbf{X}_{OE} [Fig. 1]. Hence, the blur ratio is not a fixed value belonging to an eye. The limits of resolution suggest that a blur ratio of 0.8 or less, or in rare cases up to 1.0, is needed for a letter to be resolved.

The generalized radius of a circular optotype O is \mathbf{R}_{O+} , which is in units of length and taken to be positive definite. Equation (14) and (15) are substituted into Eq. (2) and solved for \mathbf{R}_{O+} to obtain

$$\mathbf{R}_{O+} = (\mathbf{M}_{BR} \mathbf{X}_{OE})^{-1} \mathbf{W}_{OE} \mathbf{R}_{P+}. \quad (16)$$

However, optotype size is usually defined as the angle subtended by a limb of an optotype and therefore depends on the distance to the target such that [19]

$$\mathbf{R}_{K-} = -z_O^{-1} \mathbf{R}_{O+}. \quad (17)$$

\mathbf{R}_{K-} cannot be positive definite and is indeed negative definite [18,19]. \mathbf{R}_{K-} is the angular generalized radius of the optotype O and is unitless; commonly thought of as radians. Substituting

Eq. (17) into Eq. (16) we obtain

$$\mathbf{R}_{K-} = -(\mathbf{z}_O \mathbf{M}_{BR} \mathbf{X}_{OE})^{-1} \mathbf{W}_{OE} \mathbf{R}_{P+}. \quad (18)$$

To obtain the visual acuity for an eye the mean blur ratio for visual resolution is taken as 0.8 [12] and so $\mathbf{M}_{BR} = 0.8\mathbf{I}$, a scalar matrix. Similarly, surgically inserted pinhole apertures are circular and so $\mathbf{R}_{P+} = r_{P+} \mathbf{I}$ is also a scalar matrix. Equation (18) is therefore rewritten as

$$\mathbf{R}_{K-} = -\frac{r_{P+}}{z_O m_{BR}} \mathbf{X}_{OE}^{-1} \mathbf{W}_{OE}. \quad (19)$$

However, the letter that is being used is a circular optotype O, implying that \mathbf{R}_{K-} is also a scalar matrix while $\mathbf{X}_{OE}^{-1} \mathbf{W}_{OE}$ is a 2×2 matrix that may be asymmetric and is not necessarily positive definite.

Raasch [36] investigated methods to quantify astigmatic refractive error as a scalar to correlate this to visual acuity and found that vector length [37] is the best predictor. Visual acuity decreases with the length of the power vector regardless of the proportion of sphere and cross-cylinder components. The direction of the vector and, by implication axis, has little or no contribution to the visual acuity, that is, axis orientation accounts for ≤ 1 letter per line of letters [36,38–40]. Vector length is therefore a suitable model for analysing blur patches and their contribution to visual acuity.

For a 2×2 dioptric power matrix $\mathbf{F} = \begin{pmatrix} f_{11} & f_{12} \\ f_{21} & f_{22} \end{pmatrix}$ the 4×1 coordinate vector for basis $\beta = \{\mathbf{I}, \mathbf{J}, \mathbf{K}, \mathbf{L}\}$ [41] is given as

$$\mathbf{f} = \begin{pmatrix} F_I \\ F_J \\ F_K \\ F_L \end{pmatrix} = \frac{1}{2} \begin{pmatrix} f_{11} + f_{22} \\ f_{11} - f_{22} \\ f_{12} + f_{21} \\ f_{12} - f_{21} \end{pmatrix} \quad (20)$$

where F_I is the scalar coefficient, F_J is the ortho-antistigmatic coefficient, F_K is the oblique-antistigmatic coefficient and F_L is the anti-symmetric coefficient [42,43]. The first three entries of \mathbf{f} are the same as Thibos, *et al*'s. [37] power vector $\mathbf{t} = \begin{pmatrix} M & J_0 & J_{45} \end{pmatrix}^T$. The vector length is the norm of \mathbf{f} ,

$$f = \sqrt{F_I^2 + F_J^2 + F_K^2 + F_L^2} = \|\mathbf{f}\|. \quad (21)$$

2.6. Visual acuity

To resolve the problem in Eq. (19) of a scalar matrix equalling a non-scalar matrix, the vector length [Eq. (21)] of the coefficient vector [Eq. (20)] of $\mathbf{X}_{OE}^{-1} \mathbf{W}_{OE}$ for basis β is

$$r_K = \frac{r_P}{z_O m_{BR}} \|\mathbf{X}_{OE}^{-1} \mathbf{W}_{OE}\|. \quad (22)$$

r_K is the magnitude of the angular radius of the optotype O at a working distance of z_O [Fig. 1] [19]. Equation (22) makes use of the principal square root of $\mathbf{X}_{OE}^{-1} \mathbf{W}_{OE}$ and, hence, signs are ignored and only the magnitudes of r_K and r_P are used.

Visual acuity is defined as the angle subtended at the eye by a limb of a letter and is, hence, dependent on optotype size and working distance. The minimum angle of resolution (MAR) is defined as the minimum angle subtended by the individual limb of the optotype. For example,

for a 6/6 optotype O, the diameter of the letter subtends $5'$ and each limb subtends $1'$. To convert from r_K to MAR , in minutes of arc, the relationship

$$MAR = r_K \times \frac{2}{5} \times \frac{10800}{\pi} \quad (23)$$

is used and may in turn be used to obtain $\text{Log}MAR$ or Snellen notation of VA. Equation (22) is limited in that it only applies to the outline of a circular optotype O, however, Eq. (23) represents an equivalent MAR . If the human eye can interpret a blur ratio of ≤ 0.8 then Eq. (23) allows us to determine the minimum optotype size, as a MAR , that is resolvable.

2.7. Depth of field

Depth of field is modelled as the VA as a function of working distance or $r_K = f(z_O)$ which is given by Eq. (22). The dependence of r_K on z_O is not obvious. z_O is included in \mathbf{W}_{OE} [Eq. (12)] and \mathbf{X}_{OE} [Eq. (13)]. From Fig. 1, any property with the subscript OE or OA involves the working distance z_O . Using the relationship given by Eq. (22), the depth of field may be modelled for any eye, including eyes that have astigmatic elements. Equation (22) is not limited to circular pinhole apertures but may include apertures (and pupils) that may be elliptical and positioned at any longitudinal position. The optotype O may be circular or elliptical, as is found in some VA charts.

3. Results and discussion

The results for depth of field using the proposed model are illustrated graphically and the examples are based on Le Grand's four-surface eye. The monocular depth of field obtained by the three artificial intraocular pinhole apertures are compared to a naked eye with a 3 mm pupil diameter (Fig. 2 and 4 to 6). The monocular depth of field depends on the underlying refractive status and so a few examples of the model eye with myopic refractive status as well as an astigmatic status are provided (Fig. 2 to 4). The eye's chromatic difference in focus is approximately 2.1 D [44] and this is illustrated as a function of monocular depth of field (Fig. 5). And finally, monovision (binocular) depth of field is modelled according to Naeser *et al*'s. [45] suggested refractive status (Fig. 6).

3.1. Pinhole apertures

The first of the three pinhole apertures designed for surgical insertion into the eye was the KAMRATM (CorneaGen, USA) corneal pinhole inlay and has been discontinued mainly due to dissatisfaction with distance and near vision [46], however, it is included in the examples. It was surgically inserted monocularly into the corneal stroma of the non-dominant eye and needed to be decentred nasally by 0.5 mm to align with the line of sight [47,48]. The second pinhole aperture is the IC-8 IOL (AcuFocus, owned by Bausch and Lomb, USA) [3–5,49] with the pinhole aperture embedded into the front-surface of the intraocular lens. Like the KAMRA, it is intended to improve presbyopia and depth of field and is inserted monocularly in the non-dominant eye. In addition, AcuFocus recommends the IC-8 as a secondary intervention for eyes with irregular astigmatism or for the second eye when the first eye displays dysphotopsia [4]. Finally, the third pinhole aperture is primarily designed for highly irregular and optically compromised corneas when all conventional interventions have failed. The Xtrafocus 93 L pinhole is a piggyback phakic IOL (Morcher, Germany) implanted into the ciliary sulcus to piggyback with the crystalline lens or an IOL [6,7] and is no longer available, but included in the examples.

Each of the three pinhole apertures has a slightly different aperture diameter and is inserted at a different longitudinal position (Table 1). In the model eye, the KAMRA is 1.6 mm in diameter and is inserted at a depth of 200 μm in the corneal stroma, the Xtrafocus has a hole in the material of diameter of 1.3 mm and is positioned at a depth of 4.07 mm behind the cornea in the model, pushing the crystalline lens back in the process and the IC-8 IOL has a diameter of 1.36 mm and

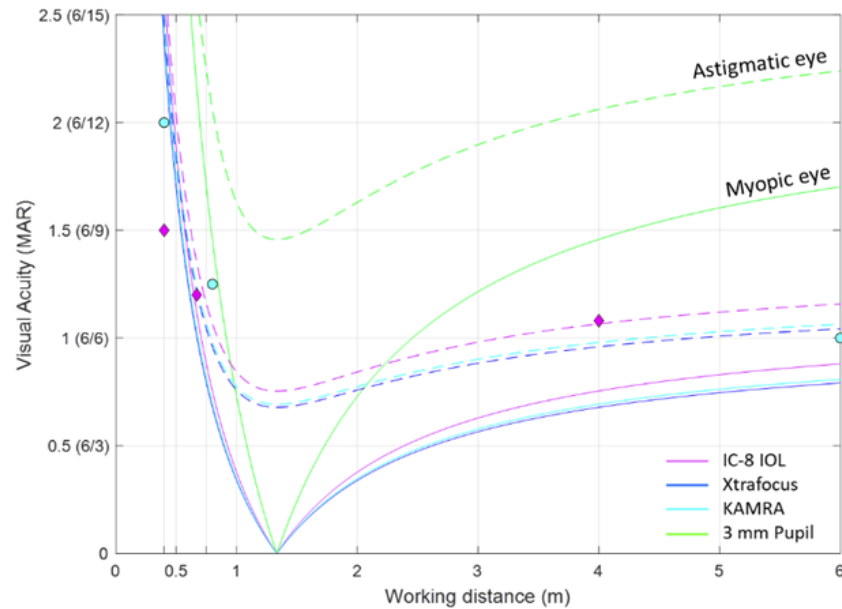


Fig. 2. Depth of field, based on a blur ratio of 0.8, for the model eye with four apertures. Solid lines indicate refractive status of 0.75 D myopia and dashed lines indicate an astigmatic refractive status of $-0.25/-1.00 \times 90$. Best VA is at 1.33 m for both the myopic and astigmatic eyes. Two unlabelled working distances are marked at 0.4 and 0.75 m. The published visual acuities are indicated in magenta diamonds for the IC-8 IOL [49] and cyan circles for the KAMRA inlay [11,47].

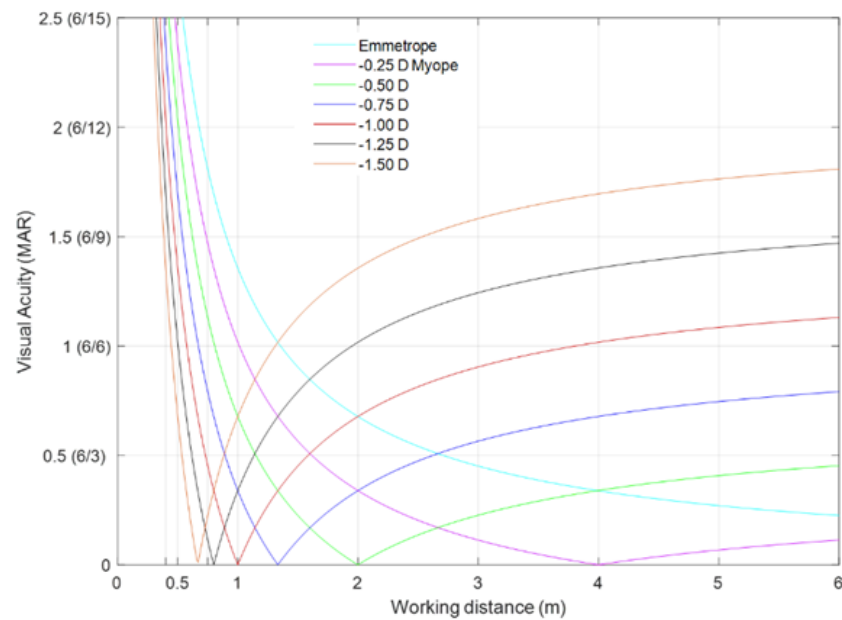


Fig. 3. Depth of field for the eye with Xtrafocus pinhole insert. The eye has been left slightly myopic, with different refractive statuses in 0.25 D steps from emmetropia to -1.50 D.

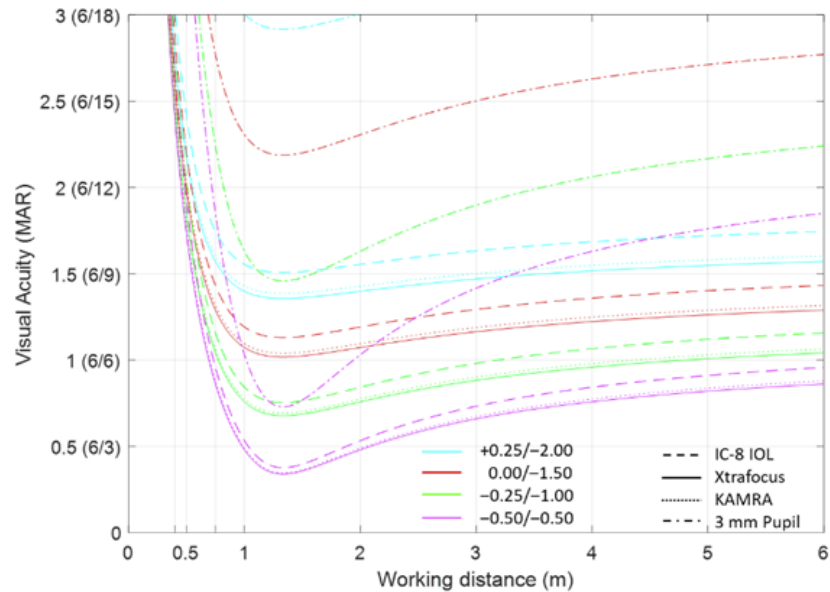


Fig. 4. Depth of field for four astigmatic refractive statuses. The four cylinder powers increase from -0.50 to -2.00 D in 0.50 D steps and are combined with spherical powers to ensure that the circle of least confusion is at 1.33 m for all four powers. The axes are at 90° , however axis makes no difference to the depth of field model. The three pinhole apertures and the naked eye with 3 mm pupil diameter are included.

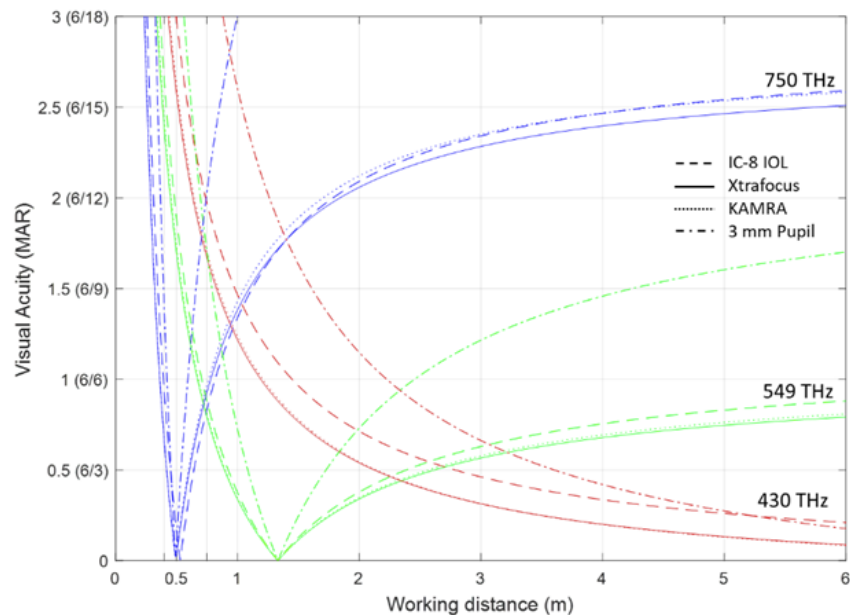


Fig. 5. The depth of field for the myopic model eye as a function of frequency, illustrating four apertures. The depth of field is shown for 750 THz (399.72 nm) in blue, 430 THz (697.19 nm) in red and a reference frequency of 549 THz (546.07 nm) in green. The eye is myopic by 0.75 D at reference frequency of 549 THz.

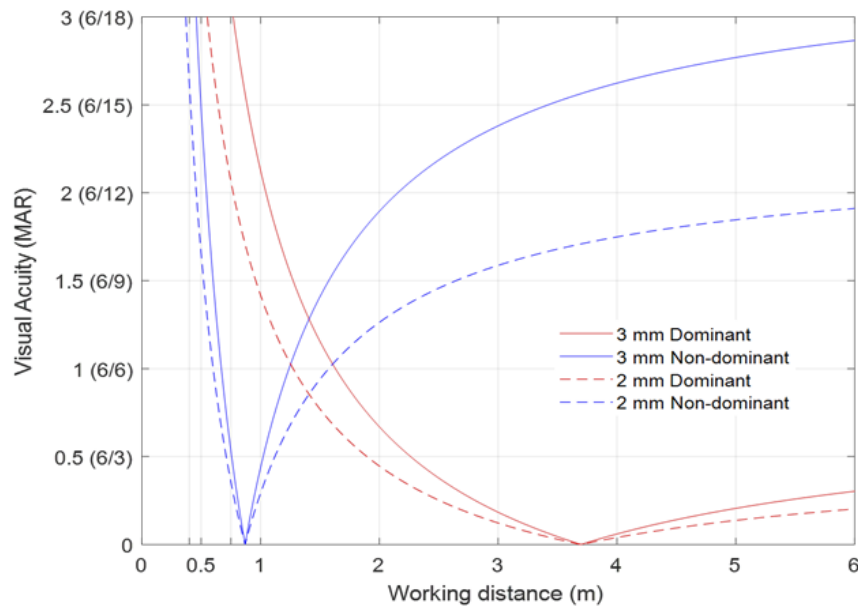


Fig. 6. The naked eye with 3 mm pupil (solid lines) and 2 mm pupil (dashed lines). The dominant eye (red) has a refractive status of -0.27 D, focussing at 3.7 m and the non-dominant eye (blue) has a refractive status of -1.15 D, focussing at 0.87 m.

Table 1. Parameters of the model eye, based on Le Grand's four-surface eye. The first corneal surface is changed to model a myopic refractive compensation of 0.75 D or astigmatism of $-0.25/-1.00 \times 90$. Homogenous refractive indices are for reference wavelength of 546.07 nm. All units of length are in mm.

Parameter	Symbol	Naked eye	KAMRA	IC-8 IOL	Xtrafocus
Cornea myopic	r_{K1}	7.7075	7.7075	7.8	7.3780
Cornea astigmatic	r_{K1}	7.7869{90} 7.6297	7.7869{90} 7.6297	7.8814{90} 7.7205	7.4507{90} 7.3067
Cornea second surface	r_{K2}	6.5	6.5	6.5	6.5
Lens first surface	r_{L1}	10.2	10.2	11.0580	10.2
Lens second surface	r_{L2}	-6.0	-6.0	-11.0580	-6.0
Thickness cornea	z_K	0.55	0.2 + 0.35	0.55	0.55
Gap anterior chamber	z_Q	3.05	3.05	6.6	4.07
Thickness lens	z_L	4.0	4.0	1.0994	4.0
Gap vitreous chamber	z_V	16.5965	16.5965	15.9471	14.9465
Index cornea	n_K	1.3782	1.3782	1.3782	1.3782
Index aqueous	n_Q	1.3378	1.3378	1.3378	1.3378
Index lens	n_L	1.4220	1.4220	1.4850	1.4220
Index vitreous	n_V	1.3373	1.3373	1.3373	1.3373
Aperture diameter	r_P	3	1.6	1.36	1.3

is positioned at a depth of 6.6 mm behind the cornea in the model. In addition, the IC-8 IOL has a higher refractive index and refractive dispersion than the crystalline lens [50].

To illustrate the depth of field, Le Grand's eye is used as a basis and the first corneal surface manipulated to simulate the effect of LASIK. Two refractive states are modelled; the first leaves

the eye 0.75 D myopic and the second leaves the eye astigmatic with a refractive compensation of $-0.25/-1.00 \times 90$. While these pinhole solutions are aimed at the presbyopic population, it is possible that recipients may still have small amounts of accommodation, with the obvious exception of the IC-8 IOL. However, the model eyes assume the absence of accommodation at all times. In Fig. 2 to 6, the refractive status at reference wavelength of 546.07 nm [51] of all four eyes is identical. The parameters used to model the three pinhole apertures are given in Table 1. Figure 6 models monovision and is the only binocular model for depth of field. (In Table 1, the radii of curvature for the astigmatic cornea are represented by $r_1 \{A_1\} r_2$ which is read as r_1 along A_1 and r_2 along $A_1 \pm 90^\circ$ [21,52].) The radii of curvature for the IC-8 IOL have been calculated to match the model and do not necessarily match any IOL available from Acufocus or IOL prediction formulae.

Figure 2 to 6 show the depth of field as the VA as a function of working distance z_O . The VA is obtained using Eq. (22) and a mean blur ratio of 0.8 is used throughout the examples. The model uses the MAR [Eq. (23)] and Snellen metric is indicated for comparison purposes. While LogMAR is usually the preferred scale for VA, MAR is chosen because the scale illustrates the depth of field more meaningfully than the scale for LogMAR. The graphs provide a clear indication of the VA achievable at any working distance.

3.2. Effect of refractive status on depth of field

An eye with a pinhole aperture implanted should be left with a refractive status that is slightly myopic. Tabernero and Artal [48] suggest between -1.00 and -0.75 D while Dick *et al.* [49] recommend -0.75 ± 0.25 D. In addition, it is claimed that the IC-8 IOL lens is very forgiving of the endpoint refraction and that it can compensate for up to 1.50 D of astigmatism, that is a -1.50 D cylinder power combined with a sphere of between 0 and 1.00 D [2–5,49].

Figure 2 shows the depth of field for the model eye with two alternate refractive states. The solid lines represent eyes that all have a myopic refractive status of 0.75 D, while the dashed lines represent an astigmatic refractive status of $-0.25/-1.00 \times 90$. The circle of least confusion is conjugate with a working distance of 1.33 m, which is the same as the far point for the myopic eye. Within the limits of visual resolution, all the optotypes for acuities above the relevant curve are resolvable. The depth of field is interpreted as the width of the working distance for the desired MAR or visual acuity above the curve. It is conceivable that different VAs are required at different working distances or tasks. For the myopic eye, the MAR approaches zero as the eye's far point is approached.

In Fig. 2 the naked eye with a myopic refractive status of 0.75 D and pupil diameter of 3 mm, is able to resolve letters of size 6/6 between the distances of 0.91 and 2.46 m. The eyes with the three pinhole apertures each have very similar near profiles; the depth of field is from 0.67 m to beyond 10 m. The astigmatic naked eye with 3 mm pupil diameter (green dashed line) does not achieve 6/6 VA at any working distance. The three eyes with pinhole apertures achieve a depth of field of from 0.77 to 4.80 m for a VA of 6/6 for the astigmatic refractive status.

The depth of field of the three pinhole apertures is superior to the naked eye with 3 mm pupil (green lines), for both the myopic (solid lines) and astigmatic (dashed lines) refractive statuses (Fig. 2). Similarly, the eyes with Xtrafocus (blue) and KAMRA (cyan) pinholes have slightly better depth of field than with the IC-8 IOL (magenta). However, the depth of field at each VA is better for the myopic eyes than for the astigmatic eyes. It appears that a small amount of astigmatism is not an advantage for increasing depth of field in eyes with pinhole apertures. This is similar to the findings of Naeser and Hjortdal [53].

A systematic review of twenty-two studies on the IC-8 IOL [9], mostly focused on clinical outcomes, included five studies that published VA results along with the mean spherical refractive error (MSRE). The VA results are presented as the percentage of participants achieving 6/9.6 (20/32) or better at three distances; near, intermediate and distance. The follow-up periods range

from 1 to 24 months in the twenty-two studies. A second systematic review [10] included eighteen studies of the KAMRA corneal inlay. Similarly, most studies concentrated on clinical findings and only five studies published VA results for three distances. The VA results were given as the percentage of participants that obtained 6/9.6 or better at near or intermediate and (6/7.5) (20/25) at distance. MSRE was not provided in the review [10] so the original articles were consulted. The studies [9,10] that provided mean VA at near, intermediate and distance with working distances and whose MSRE were provided and were closest to -0.75 D were selected for comparison with the model.

The mean monocular post-operative photopic uncorrected VA in eyes with the IC-8 inserted is 6/6.5, 6/7.5 and 6/9 for distance (4 m), intermediate (0.67 m) and near (0.4 m) at six months respectively ($n = 105$, LogMAR \pm SD given as 0.06 ± 0.15 , 0.08 ± 0.12 and 0.18 ± 0.14) [49] and for eyes with the KAMRA inlay inserted is 6/6, 6/7.5 and 6/8.5, at distance (6 m), intermediate (0.8 m) and near (0.4 m), respectively at 12 months [11,47] ($n = 478$; LogMAR \pm SD given as 0.01 ± 0.11 , 0.14 ± 0.14 and 0.18 ± 0.16 , lighting not provided [11]). The average MRSE for the IC-8 IOL at 6 months post-operatively was -0.42 ± 0.55 D, while the average sphere was -0.26 ± 0.61 D and average cylinder power was -0.37 ± 0.41 D [49]. The average MRSE for the KAMRA inlay at 12 months was $+0.27 \pm 0.37$ D [12,13]. The depth of field in the KAMRA implanted eyes was given as 3.5 D of defocus range at 6/12 (20/40) [11].

Comparison of the performance of the IC-8 and KAMRA to published results indicate that the model gives similar results for monocular, unaided VA in the non-dominant, operated eyes (Fig. 2). The published mean uncorrected VA in the eye with pinhole insert is indicated in Fig. 2 for the KAMRA inlay with cyan circles [11,47] and for the IC-8 IOL with magenta diamonds [11]. The model indicates better VA at distance and intermediate working distances, while at near the KAMRA and IC-8 appear to provide better VA than the model's predicted results. This is possibly due to accommodation in the KAMRA inlay cohort. The mean \pm SD age for the KAMRA inlay at time of surgery was 52.2 ± 3.2 years [47] and for the IC-8 IOL was 51.5 ± 3.6 years [11]. The Xtrafocus is intended for eyes with optically compromised corneas and so no published depth of field results were found for this pinhole. Published results vary between studies, surgeons, inclusion criteria, time after surgery as the eye heals and settles and, in particular, refractive endpoints have a strong influence on results [9].

Figure 3 illustrates the depth of field for a range of myopic refractive statuses from emmetropia to 1.50 D myopia in 0.25 D steps for the eye with a Xtrafocus piggyback aperture inserted. It is no surprise that the greater the myopia, the better the VA at near and the worse the VA at distance. The gain in working distance at near, by increasing the myopic refractive status, is small, compared to the potential loss of VA at distance. The blue line (0.75 D myopia) appears to give the best compromise; that is, better than 6/6 at distance. It is the same as the solid blue line in Fig. 2. This supports the results found by Tabernero *et al.* [48] and Dick *et al.* [49]. While Fig. 3 is based on the Xtrafocus aperture, the results are similar for the other two pinhole apertures (compare Fig. 2).

Figure 4 gives the depth of field for the model eye with four apertures; the three pinholes and the naked eye with 3 mm pupil diameter. Four astigmatic refractive statuses are modelled, with cylinder powers from -0.50 to -2.00 D in -0.50 D steps. The spherical powers are adjusted such that the circle of least confusion always falls at 1.33 m to aid comparison. The green lines represent $-0.25/-1.00 \times 90$ which is the same power as the dashed lines in Fig. 2. The best VA is at 1.33 m and gently reduces to the right as the target extends into the distance. The VA reduces rapidly to the left into the near vision region. The three eyes with pinhole apertures all achieve better VA than the naked eye with 3 mm pupil diameter. The model confirms the claim [49] that patients with the IC-8 IOL will tolerate up to -1.50 D of cylinder power for unaided intermediate and near vision, with a visual outcome of 6/9. Computational eye models found that for a pupil

of 3 mm diameter, the same eye could tolerate twice as much astigmatism (cylinder lens power) with the 1.6 mm diameter KAMRA inlay to obtain the same VA [54].

Pinholes are expected to be forgiving of residual astigmatism. A computational eye model [54] predicted that an eye with the KAMRA corneal inlay (with a pinhole aperture of 1.6 mm diameter) will tolerate twice as much astigmatism (cylinder lenses placed at a 15 mm vertex distance) as the same eye with a 3 mm pupil diameter. In Fig. 4 this is seen at approximately 1.33 m, but not at near and distance. Clinically, the eyes that had the IC-8 IOL implanted could tolerate up to 1.5 D of residual astigmatism (negative cylinder) when combined with a sphere of between 0 and 1 D [49].

3.3. Effect of chromatic difference in focus on depth of field

The chromatic difference in focus (CDF) across the visible light spectrum is approximately 2.1 D for the emmetropic human eye [44]. This may provide a different perspective to depth of field. Figure 5 shows the depth of field for three visible light frequencies, that is, blue at 750 THz (399.72 nm), red at 430 THz (697.19 nm) and a reference frequency of green at 549 THz (546.07 nm). The model eye is myopic (−0.75 D) at reference wavelength 546.07 nm and is shown for four apertures. The green lines are the same as the solid lines illustrated in Fig. 2.

Unsurprisingly, the blue light focusses closer to the eye (0.363 m) than the reference green light (1.33 m) and the red light focuses at >9.5 m, which extends beyond the graph. The blue light has a much shallower depth of field than the green and red light. The IC-8 IOL has a different chromatic dispersion [50,55] to the crystalline lens and so the far point for the blue and red light is slightly different to that for the three phakic model eyes. For the three pinhole apertures and 6/6 VA, the blue light gives a gain of 31 cm compared to the green light. There is an overlap between the blue and green light in the intermediate distance region and again an overlap between the green and red in the distance vision range.

3.4. Monovision and depth of field

Naeser *et al.* [45] proposed that the ideal refractive status for monofocal pseudophakic monovision should be 0.27 D myopia in the dominant eye and 1.15 D myopia in the non-dominant eye. This gives spectacle independence for distance and intermediate vision with minimal binocular interference. Figure 6 shows Naeser *et al.*'s [45] monovision system for Le Grand's eye with a 3 mm pupil (solid lines) and 2 mm pupil (dashed lines). For the 2 mm pupil, the dominant eye resolves 6/6 from 1.275 m into the distance, while the non-dominant eye's depth of field is from 0.6 m proximally to 1.575 m distally. Whilst there is a 30 cm binocular [45] overlap between 1.275 and 1.575 m where both eyes can resolve 6/6, there is a monovision depth of field from 0.6 m to distance.

When the pupil dilates to 3 mm, the depth of field is shallower for each eye. For the 6/6 and 6/7.5 sized letters, there is no binocular overlap region. The smallest letters allowing a binocular overlap are the 6/9 letters. The dominant eye with 3 mm pupil can resolve 6/9 letters from 1.275 m into the distance and the non-dominant eye resolves 6/9 letters at near between 0.6 m and 1.575 m allowing for an intermediate binocular overlap of 0.3 m between 1.275 m and 1.575 m whilst providing a monovision depth of field from 0.6 m to distance, the same as the 2 mm pupil provided for the 6/6 letter size.

Equation (22), indicates what a change in aperture size or blur ratio will have on the depth of field in each of Fig. 2 to 6. A change in pupil or pinhole diameter r_p results in a graph that shifts the curves up or down (for astigmatic curves) or widens or narrows for the myopic curves. The change in depth of field due to pupil size is illustrated in Fig. 6 for the myopic eye. The positions of the curves for the different pinholes in Fig. 2 are due to design differences in aperture sizes and longitudinal positions among the three surgically insertable pinhole apertures.

The blur ratio m_{BR} represents blur interpretation of an eye and varies among individuals. A change in m_{BR} , for example from the mean of 0.8 to 1.0, will result in the depth of field curves dropping and widening so that VA improves at all distances and consequently depth of field improves, and *vice versa*.

In Fig. 2 to 5, the four apertures that were compared were at different longitudinal positions and also had different aperture sizes. When all four apertures are made the same size, the effect of the depth of field curves is that the corneal inlay gives the best VAs and depth of field, followed by the pupil, then the Xtrafocus and then the IC-8 IOL, in order from anterior to posterior.

3.5. Limitations

The factors relating to first-order optics are working distance and letter size, that is, angle subtended by the optotype O at the eye. The model is based in linear optics and therefore the usual limitations of first-order optics apply. Higher-order aberrations are ignored. The limitations of diffraction may be ignored, provided the pinhole is larger than 0.5 mm [13]. A number of factors are not accounted for, these include luminance, contrast, spectral profile and colour (except Fig. 6), accommodation, field of view, misalignment and vignetting. We make the valid assumption that the pinhole aperture is the limiting aperture for the eye and that the eye's pupil is sufficiently large for the pinhole aperture to be the limiting aperture, but small enough to avoid vignetting beyond the outer diameter of the mask creating the artificial pinhole aperture.

Blur interpretation varies among individuals. The model is based on a mean blur ratio of 0.8, however blur ratio varies among individuals from 0.66 to 1.0 [12–14]. The model is also based on the assumption that there is no accommodation, and that the surgeries are “perfect”, that is, no misalignment, complications, or other ocular conditions. Only a circular or elliptical optotype O is quantifiable as a matrix. The results are approximated to letters in general.

A further limitation is that the effects of transverse displacement of pinhole apertures is not included in this study. These transverse effects are exaggerated the further from the iridial plane the pinhole is inserted.

4. Conclusion

Depth of field in eyes, including eyes with astigmatic elements and pupils or artificial apertures that may be elliptical is modelled as the VA as a function of working distance. The model obtained in this study illustrates the depth of field as the working distance range across which the desired visual acuity is achievable. The model includes eyes that have astigmatic elements, and pupils or apertures that are elliptical and artificial intraocular pinhole apertures at varying longitudinal positions within the eye or system. By defining the depth of field as the VA dependent on the working distance, it is possible to predict the visual acuity at any particular working distance and is not limited to the three testing distances of near, intermediate and distance.

Visual acuity is given by Eq. (18), however, Eq. (22) is more useful because of the physical limitations of the design of letters on VA charts. VA is dependent on working distance, pupil or aperture geometry, longitudinal position of the aperture as well as the optics of the eye. The closer the pinhole aperture is implanted to the eye's corneal plane, the greater the tolerance to residual refraction, including astigmatism.

Visual acuity and depth of field are closely related. The required VA may vary according to working distance and the task at hand. It is conceivable that different visual acuities are required at different working distances and for different tasks. The improvements in visual acuity created by a pinhole are related to the blur patch geometry (size, shape and orientation) on the retina and not to any change in the reduced vergence at the retina.

Depth of field is dependent on working distance and visual acuity, which, in turn, is dependent on the pupil or aperture geometry (size and shape) and the optics of the eye, which, together affect

the geometries of the blur patches and the image. By implication, the depth of field is affected by the residual refraction (Fig. 2 to 6), the individual's blur ratio and the colour of the target (Fig. 5).

A small amount of residual myopia [19,48] is an advantage to increasing the depth of field on the near-vision end of the field without interfering with the distance-vision end of the field in sufficiently small pinhole apertures (Fig. 3). Depth of field depends on the visual acuity required and is a function of a near-emmetropic or slightly myopic eye. Depth of field is a function of good visual resolution (relating to the eye's own maximum resolvable blur ratio) and a near-emmetropic (or slightly myopic) eye.

From Fig. 2, it is clear that residual astigmatism is not an advantage to increase depth of field without compromising VA at all distances. AcuFocus claim that the IC-8 will allow the eye to tolerate up to 1.5 D of cylinder astigmatism [2–5,49]. From Fig. 4, the curves for refractive status 0.00/–1.50 \times 90 allow for 6/7.5 VA at distance (6 m) and intermediate (0.8 m) working distances and 6/15.5 at near (0.4 m), which may be acceptable for some patients.

The graphs provide a clear prediction tool of potential depth of field for patients; surgeons, researchers and even a teaching tool for students. The simplicity of the graphs makes it easy to read and understand. Depth of field is given in units of length instead of dioptres, making it suitable for illustrating depth of field to the general public. Equation (22) provides the depth of field to be modelled graphically as the VA as a function of working distance. The graphs give an indication of the VA achieved at any desired working distance. In addition to depth of field and VA, comparison between different aperture or pinhole sizes, longitudinal positions of aperture insertion, colour (chromatic depth of field), blur ratios, refractive errors, including astigmatism and even monovision outcomes are easy to model and understand. In astigmatic eyes, the VA and the position of the circle of least confusion and the drop-off in VA as a target is moved closer or further from the eye, either physically, or with lenses, is easy to predict from the graph.

Funding. University of Johannesburg (Global Excellence Scholarship).

Acknowledgements. This study was part of a higher degree under the supervision of WF Harris and A Rubin. It was presented at VPO 2022, Cambridge. I thank WFH and AR for discussions and WFH and C Troskie-de Bruin for reading and commenting on the manuscript. I thank M Simpson for drawing my attention to Ref. [8].

Disclosures. The author declares that there are no conflicts of interest related to this article.

Data availability. No data were generated or analyzed in the presented research. The eye model is based on parameters provided in Table 1.

References

1. OIS. Sightlife Surgical CEO Monty Montoya says start-up is building out cornea market. OIS Podcast, episode 177. <https://ois.net/sightlife-surgical-ceo-monty-montoya-says-start-building-cornea-market/>.
2. N. Tarantino, AcuFocus slideshow (OIS 5 May 2015). <https://www.slideshare.net/Healthegy/spotlight-on-the-premium-channel-acufocus-61999560>.
3. Acufocus. IC-8 Small aperture IOL. <http://www.acufocus.com/int/sites/default/files/MK-1268%20Rev%20B%2C%20IC-8%20IOL%20Physician%20Brochure.pdf>.
4. Y. Mitchell, Acufocus – OIS@ ASCRS (2018). OIS.net. https://www.youtube.com/watch?v=Wpec71Lugmc&utm_source=OIS+Newsletter&utm_campaign=031fd01d7e-OIS_Newsletter_COPY_01&utm_medium=email&utm_term=0_1aaae0a1fa-031fd01d7e-282185169.
5. Acufocus. IC-8 Physician brochure. <http://www.acufocus.com/int/sites/default/files/MK-1268%20Rev%20C%2C%20IC-8%20IOL%20Physician%20Brochure.pdf>.
6. C. Trindade, "Development of a pinhole implant: XtraFocus," *Cataract Refract. Surg. Today: Europe*, February (2016).
7. Morcher. <http://www.morcher.com/nc/en/products/special-implants.html>.
8. O. Kermani, H. B. Dick, and H. Lubatschowski, "Femtomasking: laser-generated apertures to extend depth of focus and reduce optical aberrations in intraocular lenses," *J. Cataract Refract. Surg.* **48**(9), 1095–1096 (2022).
9. J. Sánchez-González, M. C. Sánchez-González, C. De-Hita-Cantalejo, and A. Ballesteros- Sánchez, "Small aperture IC-8 extended-depth-of-focus intraocular lens in cataract surgery: a systematic review," *J Clinl Med.* **11**(16), 4654 (2022).
10. I. Pluma-Jaramago, C. Rocha-de-Lossada, R. Rachwani-Anil, and J. Sánchez-González, "Small apertura intracorneal inlay implantation in emmetropic presbyopic patients: a systematic review," *Eye.* **36**(9), 1747–1753 (2022).

11. J. A. Vukich, D. S. S. Durrie, J. S. Pepose, V. Thompson, C. van de Pol, and L. Lin, "Evaluation of the small-aperture intracorneal inlay: Three-year results from the cohort of the U," *S. Food and Drug Administration clinical trial. J Cataract Refract Surg.* **44**(5), 541–556 (2018).
12. R.B. Rabbetts, *Bennett & Rabbetts' Clinical Visual Optics*, 4th ed. (Butterworth-Heinemann-Elsevier, 2007), Chap. 4, p. 15.
13. R. R. J. Jacobs, I. L. Bailey, and M. A. Bullimore, "Artificial pupils and Maxwellian view," *Appl. Opt.* **31**(19), 3668–3677 (1992).
14. G. Chan, G. Smith, and R. J. Jacobs, "Simulating refractive errors: source and observer methods," *Am. J. Optom. and Physiol. Opt.* **62**(3), 207–216 (1985).
15. V. Guillemin and S. Sternberg, *Symplectic Techniques in Physics* (Cambridge University Press, 1984), pp. 4–7.
16. D.A. Atchison and G. Smith, *Optics of the Human Eye* (Butterworth-Heinemann, 2000), pp. 79–86, 213–220.
17. W. F. Harris, "Aperture referral in heterocentric astigmatic systems," *Ophthalmic Physiol Opt* **31**(6), 603–614 (2011).
18. T. Evans and W. F. Harris, "Vector space of generalized radii of ellipses for quantitative analysis of blur patches and other referred apertures in the astigmatic eye," *J. Opt. Soc. Am. A* **36**(4), B93–B96 (2019).
19. T. Evans, "Linear optics of eyes with pinhole apertures," (Doctoral Thesis, University of Johannesburg, 2018).
20. V. Guillemin and S. Sternberg, *Symplectic Techniques in Physics* (Cambridge University Press, 1984).
21. T. Evans and A. Rubin, "Linear optics of the eye and optical systems: a review of methods and applications," *BMJ Open Ophthalmol.* **7**(1), e000932 (2022).
22. W. F. Harris, "The four fundamental properties of Gaussian optical systems including the eye," *S. Afr. Optom.* **58**, 69–79 (1999).
23. M. P. Keating, "A system matrix for astigmatic optical systems: II. Corrected systems including an astigmatic eye," *Am. J. Optom. Physiol. Opt.* **58**(11), 919–929 (1981).
24. M. P. Keating, "A system matrix for astigmatic optical systems: I. Introduction and dioptric power relations," *Am. J. Optom. Physiol. Opt.* **58**(10), 810–819 (1981).
25. T. M. Jeong, D.-K. Ko, and J. Lee, "Generalized ray-transfer matrix for an optical element having an arbitrary wavefront aberration," *Opt. Lett.* **30**(22), 3009–3011 (2005).
26. M. V. Pérez, C. Bao, M. T. Flores-Arias, M. A. Rama, and C. Gómez-Reino, "Description of gradient-index crystalline lens by a first-order optical system," *J Opt. A: Pure Appl. Opt.* **7**(3), 103–110 (2005).
27. W. F. Harris, "Paraxial ray tracing through noncoaxial astigmatic optical system, and a 5×5 augmented system matrix," *Optom. Vis. Sci.* **71**(4), 282–285 (1994).
28. M.P. Keating, *Geometric, Physical, and Visual Optics*. 2nd ed. (Butterworth-Heinemann, 2002). Chap. 325–345, 435–438.
29. W. F. Harris, "A unified paraxial approach to astigmatic optics," *Optom. Vis. Sci.* **76**(7), 480–499 (1999).
30. W.F. Harris, "Symplecticity and relationships among the fundamental properties in linear optics," *S. Afr. Optom.* **69**, 3–13 (2010).
31. W. F. Harris, "Magnification, blur, and the ray state at the retina for the general eye with and without a general optical instrument in front of it: 2. Near objects," *Optom. Vis. Sci.* **78**(12), 901–905 (2001).
32. D.S. Bernstein, *Matrix Mathematics; Theory, Facts and Formulas with Application to Linear Systems Theory* (Princeton University Press, 2005). Chap. 2.7.
33. W. F. Harris, "Generalized magnification in visual optics. Part 1: Magnification as linear transformation," *S. Afr. Optom.* **69**, 109–122 (2010).
34. M. H. Pincus, "Unaided visual acuities correlated with refractive errors," *Am. J. Ophthalm.* **29**(7), 853–858 (1946).
35. H. B. Peters, "The relationship between refractive error and visual acuity at three different age levels," *Am. J. Optom. Arch. Am. Acad. Optom.* **38**(4), 194–198 (1961).
36. T. W. Raasch, "Spherocylindrical refractive errors and visual acuity," *Optom. Vis. Sci.* **72**(4), 272–275 (1995).
37. L. N. Thibos, W. Wheeler, and D. Horner, "Power vectors: An application of Fourier analysis to the description and statistical analysis of refractive error," *Optom. Vis. Sci.* **74**(6), 367–375 (1997).
38. A. Rubin and W. F. Harris, "Closed surfaces of constant visual acuity in symmetric dioptric power space," *Optom. Vis. Sci.* **78**(10), 744–753 (2001).
39. L. Remón, M. Tornel, and W. D. Furlan, "Visual acuity in simple myopic astigmatism: influence of cylinder axis," *Optom. Vis. Sci.* **83**(5), 311–315 (2006).
40. L. Remón, J. A. Monsoriu, and W. D. Furlan, "Influence of different types of astigmatism on visual acuity," *J Optom* **10**(3), 141–148 (2017).
41. W. F. Harris, "Inner product spaces of dioptric power and of fundamental and derived properties of optical systems," *S. Afr. Optom.* **62**, 114–118 (2003).
42. W. F. Harris, "Power vectors versus power matrices, and the mathematical nature of dioptric power," *Optom. Vis. Sci.* **84**(11), 1060–1063 (2007).
43. W. F. Harris and R. D. van Gool, "Thin lenses of asymmetric power," *S. Afr. Optom.* **68**, 52–60 (2009).
44. T. Evans and W. F. Harris, "Dependence of the transference of a reduced eye on frequency of light," *S. Afr. Optom.* **70**, 149–155 (2011).
45. F. K. Naeser, JØ Hjortdal, and W. F. Harris, "Pseudophakic monovision: optimal distribution of refractions," *Acta Ophthalmol* **92**(3), 270–275 (2014).

46. M. Moshirfar, C. Lau, N. A. Chartrand, M. T. Parsons, S. Stapley, N. Bundogji, Y. C. Ronquillo, S. H. Linn, and P. C. Hoopes, "Explantation of KAMRA corneal inlay: 10-year occurrence and visual outcome analysis," *Clin. Ophthalmol.* **16**, 3327–3337 (2022).
47. A. K. Dexl, O. Seyeddain, W. Riha, M. Hohensinn, T. Rückl, V. Reischl, and G. Grabner, "One-year visual outcomes and patient satisfaction after surgical correction of presbyopia with an intracorneal inlay of new design," *J. Cataract. Refract. Surg.* **38**(2), 262–269 (2012).
48. J. Tabernero and P. Artal, "Optical modelling of a corneal inlay in real eyes to increase depth of focus: Optimum centration and residual defocus," *J. Cataract Refract. Surg.* **38**(2), 270–277 (2012).
49. H. B. Dick, M. Piovella, J. Vukich, S. Vilupuru, and L. Lin, "Prospective multicentre trial of a small-aperture intraocular lens in cataract surgery," *J. Cataract Refract. Surg.* **43**(7), 956–968 (2017).
50. Benz Research and Development. Intraocular Lens Materials & Manufacturing Technology 2017. <http://benzrd.com/ts/manual/#p=1>.
51. ISO 11979-2:1999 Ophthalmic Implants – Intraocular Lenses. Part 2 Optical properties and test methods.
52. W. F. Harris, "Interconverting the matrix and principal-meridional representations of dioptric power and reduced vergence," *Ophthalmic. Physiol. Opt.* **20**(6), 494–500 (2000).
53. F. K. Naeser and JØ Hjortdal, "Optimal refraction with monofocal intraocular lenses: no beneficial effect of astigmatism," *Acta Ophthalmol.* **89**(2), 111–115 (2011).
54. A. Vilipuru, J. Tabernero, and P. Artal, "Tolerance to astigmatism with a small aperture corneal inlay," *Invest. Ophthalmol. Vis. Sci.* **54**, 4280 (2013).
55. E. R. Villegas, L. Carretero, and A. Fimia, "Le Grand eye for the study of ocular chromatic aberration," *Ophthalmic Physiol. Opt.* **16**(6), 528–531 (1996).